

# Characterization of an Inertial Micro Gripper Based on Adhesion Forces

M. Dafflon, B. Lorent, W. Driesen, Prof. R. Clavel

Laboratoire de Systèmes Robotiques (LSRO)  
Ecole Polytechnique Fédérale de Lausanne (EPFL)  
Lausanne, Switzerland  
[melanie.dafflon@epfl.ch](mailto:melanie.dafflon@epfl.ch)

**Abstract** – Adhesive forces become predominant in the micro world comparing to the gravity effect implying the development of new micro manipulation strategies. This paper presents the design and conception of a gripper that use the inertial principle for the release (applying a high acceleration, in the order of 10'000g) and the adhesion for catching a micro part of 50 $\mu$ m with the goal of precisely control the position after release. Experiments were conducted and showed a positioning repeatability of 2 $\mu$ m to 6 $\mu$ m depending on the relative humidity with a success rate of more than 90%.

**Index Terms** – micro gripper, micro manipulation, dynamical effects, adhesion forces.

## I. INTRODUCTION

Microsystems can be a combination of several elements with different shapes, sizes and material and are not always produced through similar process. The necessity to assemble them with care and precision and sometimes with constraining environmental conditions requires the development of different principles of manipulation. Catching and releasing a micro object have thus been explored by researchers which have proposed many different tools. Micro tweezers as well as vacuum tools have been proposed based on the miniaturization of common macro gripper principles but adapted to the micro scale through compact and innovative actuators and processes compatible with the microsystems to assemble [1]. As adhesive effects become dominant compared to the gravity in the micro scale, they can be either a disturbance, which is looking to be overcome or minimized, or a grasping principle [2]. In this last case it is necessary to provide the gripper another release principle. By implying a high acceleration to the micro object, so by using its inertia, Haliyo et al. [3] showed the possibility to release the object and even to eject them one by one. Driesen et al. [4] implemented on collaborating mobile micro robots several strategies of pick and release based on adhesion and inertia effects as well as strategies for transferring the micro object from one tool to another.

This paper presents the integration of an inertial based micro gripper on a micro manipulation setup for pick and place operations. Measurements of positioning capabilities and reliability were conducted while varying the environmental conditions. The micro manipulation setup is described in the next section. Section III presents the

modeling of the gripping and releasing principles. Section IV discusses the design of the inertial micro gripper. Pick and release operations are then presented based on experiments. Finally a concept of passive inertial micro grippers is exposed (section VI). The last section summarizes the main results and concludes.

## II. MICRO MANIPULATION SETUP

The micro manipulation setup was designed with the goal of integrating different kinds of manipulation tools and in order to test them in variable conditions with the possibility to measure their positioning capabilities and their reliability.

The setup [5] is based on the three degrees of freedom Delta<sup>3</sup> robot with strokes of  $\pm 2$ mm and positioning repeatability of  $\pm 10$ nm thanks to its flexure hinges based structure and contact-less actuators and sensors. A standardized interface allows to mount different kinds of micro grippers on the Delta<sup>3</sup> and to place their end-effectors directly in the field of view of the microscope. In order to protect the workspace against air flows it is enclosed in a chamber where the relative humidity can also be lowered by injecting nitrogen (fig. 1).

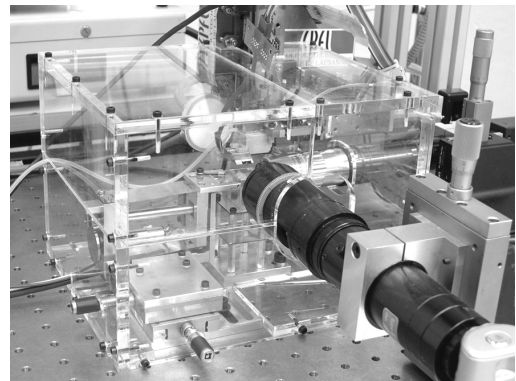


Fig. 1 Overview of the micromanipulation setup

The operation of manipulation can be fully automated based on computer vision or operated in telemanipulation. A first microscope provides a bottom view of 470 x 350 $\mu$ m<sup>2</sup> and an image pixel size of 460nm based on a Mitutoyo 10x objective. This view serves to the object and tip detection and localization. Calibration of the microscope and measurement algorithm through a precise grid of 50 $\mu$ m marks gave a final

accuracy of 200nm. The second microscope gives the lateral view through a camera mounted on a video zoom lens with magnification of 3x to 28x giving a field of view of 1.61x1.21 mm<sup>2</sup> to 0.17x0.13 mm<sup>2</sup> (Marcel Aubert system). This view serves as a fine supervision for alignment purpose and preparation procedure by the operator.

### III. GRIPPING AND RELEASE FORCES MODELING

The presented “inertial micro gripper” is based on the adhesion forces: the catching of the part is done by coming in contact with a micro object that lies on a substrate. Releasing will be executed by inducing a high acceleration to the part by the use of a piezoelectric element to counterbalance the adhesion forces.

Adhesive effects are due to intermolecular potential (Van der Waals Forces) as well as capillarity and electrostatic effects. As they become predominant at the micro scale comparing to the gravity effect, a minimal force, called pull-off force, is necessary to detach a micro object from a surface. For a contact between a sphere of radius  $R$  and a plane this force can be expressed using the JKR contact theory [6] as:

$$F = \frac{3}{2} \pi R W_{12} \quad (1)$$

$W_{12}$  is the work of adhesion between two mediums expressed with the interfacial energy  $\gamma_{12}$  and the surfaces energy of both micro object  $\gamma_1$  and tool or substrate  $\gamma_2$ :

$$W_{12} = \gamma_1 + \gamma_2 - \gamma_{12} \approx 2\sqrt{\gamma_1\gamma_2} \quad (2)$$

To be able to catch a part it is thus necessary to have two different materials on the substrate and on the tool and this with a higher surface energy on the tool. The material of the substrate is glass as determined by the setup, but a hydrophobic coating (Perfluorosilane<sup>1</sup>) was deposited on it to reduce its surface energy. The gripping zone is a glass sphere ( $\varnothing$  250 $\mu$ m). By this way the tip is detectable on the microscope field of view and gives an easy access to the part to manipulate. The contact is then sphere-sphere instead of sphere-plane, but the spherical tip was chosen to be as big as possible (still smaller than the field of view) in order to have a contact as much equivalent as possible to a plane. The equivalent radius is expressed as:

$$R_{eq} = \frac{R_{part} R_{tool}}{R_{part} + R_{tool}} \quad (3)$$

The pull-off forces of a Polystyrene ball of 50 $\mu$ m to the substrate and the end-effectors can be calculated with equation (1), combined with (3) in case of the end-effectors:

$$F_{object-substrate} = 5.24\mu\text{N}$$

$$F_{object-gripper} = 6.48\mu\text{N}.$$

<sup>1</sup> The hydrophobic coating is a Perfluorosilane provided by the Nanostructuring Research Group (NRG) at the Advance Photonic Laboratory (APL) in EPFL

	Perfluorosilane	Soda glass	Polystyrene
Surface energy (mJ/m <sup>2</sup> )	15	30	33

TABLE I  
SURFACE ENERGY FOR THE MATERIALS INVOLVED IN THE EXPERIMENTS

To release the part a high acceleration has to be applied. Based on the pull-off force modeled by JKR, the minimal acceleration to release the part is calculated as:

$$a = \frac{F_{pull-off}}{m} = \frac{\frac{3}{2} \pi R_{eq} W_{12}}{\frac{4}{3} \pi R_{object}^3 \rho} = \frac{9 W_{12} R_{eq}}{8 R_{object}^3 \rho} \quad (4)$$

The minimal acceleration to release a Polystyrene ball of 50 $\mu$ m ( $\rho_{Polystyrene} = 1.05 \cdot 10^3$  kg/m<sup>3</sup>) is thus  $8.99 \cdot 10^4$  m/s<sup>2</sup>.

### IV. GRIPPER DESIGN AND MODELING

The gripper consists of a steel beam ( $8 \times 4 \times 0.5$  mm<sup>3</sup>, 125 mg) that is clamped on the one end and has a piezoelectric actuator ( $4 \times 3 \times 1$  mm<sup>3</sup>, 94 mg) attached to it on the other end (see figure 2). A small piece of silicon ( $1 \times 3 \times 0.2$  mm<sup>3</sup>, 1.4 mg) is attached to the piezoelectric actuator, to which a glass sphere ( $\varnothing$  250 $\mu$ m) has been attached, which allows for grasping a micro object without crushing all the objects that are lying around it. The interface of manipulation (i.e. the sphere) is thus rigidly fixed just below the piezoelectric actuator. Compared to a configuration with a silicon cantilever, this configuration has the advantage of generating an acceleration that is as vertical as possible, which should result in a better precision during the release operation.

The first resonance frequency of the gripper has been calculated to be in the range of a few kHz. As typical excitation frequencies used in the experiments go from 150 to 350 kHz, this resonance mode (as well as the higher modes) is supposed not to be excited.

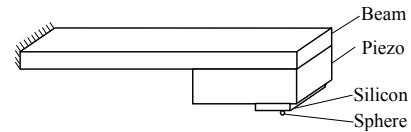


Fig. 2 Gripper design

In general the acceleration supplied by a single layer piezoelectric actuator working in  $d_{33}$  mode and with sinusoidal excitation is expressed as:

$$a = \Delta z_{amp} \cdot \omega^2 = \eta \cdot U \cdot d_{33} \cdot (2\pi f)^2 \quad (5)$$

with  $\Delta z_{amp}$  the amplitude of piezoelectric displacement,  $U$  the applied voltage,  $f$  frequency,  $\omega$  pulsation and  $d_{33}$  the piezoelectric coefficient ( $d_{33}=450 \cdot 10^{-12}$  m/V for PIC 151 from Physik Instrumente, GmbH). The coefficient  $\eta$  has been added in order to take into account the different causes of attenuation of the piezoelectric displacement discussed below.

As the piezoelectric actuator is excited far above the resonance frequency of the whole system, the elastic force in the beam is negligible compared to the inertial forces. Hence, in order to obtain an equilibrium in inertial forces, a fraction

$\alpha t$  of the total thickness  $t$  of the piezo (see figure 3) will participate to the acceleration of the beam, while only the fraction  $\beta t$  contributes to generation of the desired acceleration of the micro object that is sticking to the gripper. Consequently, part of the displacement of the piezoelectric actuator will be lost in the deformation of the beam. The value of these fractions  $\alpha$  and  $\beta$  are calculated by considering an effective length of the beam that is only  $\frac{1}{3}$  of its physical length as the deformation of the beam is approximated by a quadratic function. The weight of the piece of silicon and the sphere are neglected.

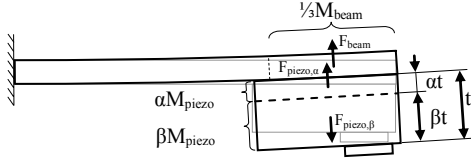


Fig. 3 Displacement absorbed by deflection of the beam and equilibrium of upward and downward inertial forces

The fractions  $\alpha$  and  $\beta$  are calculated by finding the vertical position inside the piezo where there is equilibrium between upward and downward vertical acceleration (see figure 3):

$$F_{beam} + F_{piezo, \alpha} = F_{piezo, \beta} \quad (6)$$

The amplitude of the inertial force on a mass  $M$  generated by a sinusoidal vibration with amplitude  $A$  equals  $A\omega^2 M$ . The pulsation  $\omega$  is the same for the three forces and the displacement generated by a fraction of the piezo actuator is proportional to the thickness of this fraction. So equation (6) can also be written as:

$$\frac{\alpha t}{3} M_{beam} + \frac{\alpha t}{2} \cdot \alpha M_{piezo} = \frac{\beta t}{2} \cdot \beta M_{piezo} \quad (7)$$

The two factors  $\frac{1}{2}$  are due to the fact that the center of gravity of each fraction of the piezo is in the middle of this fraction, so the displacement of the center of gravity is only half of the total deformation of each piezoelectric fraction. Given that  $\alpha + \beta = 1$ , equation (7) can be easily solved to  $\alpha = 0.35$ ,  $\beta = 0.65$ . So it can be concluded that 35% ( $\eta_1 = 0.65$ ) of the displacement of the piezo is lost into the deflection of the beam.

The frequency of the resonance mode in which the piezo is excited in the axial direction is more complicated to calculate and is not treated in this paper. However, a lower limit to this frequency can easily be obtained by calculating the axial resonance mode of the piezo in a perfectly clamped boundary condition, which would correspond to a steel beam with an infinite mass. This resonance frequency is calculated by considering the axial stiffness ( $k_{piezo}$ ) of the piezo and an effective mass ( $M_{piezo, eff}$ ) that is one third of the physical mass:

$$f_{piezo} = \frac{1}{2\pi} \sqrt{\frac{k_{piezo}}{M_{piezo, eff}}} = \frac{1}{2\pi} \sqrt{\frac{E_{piezo} S/t}{1/3 M_{piezo}}} = 804 \text{ kHz} \quad (8)$$

in which  $E_{piezo}$  is the Young modulus of the piezoceramics ( $E_{piezo} = 66.7 \text{ GPa}$ ) and  $S$  the section ( $S = 4 \times 3 \text{ mm}^2$ ). In reality the mass of the steel beam is not infinite which will move the plane of no vertical displacement from the upper edge of the piezo to inside the piezo, which will result into an increase of the resonance frequency. The frequency range used in the experiments (150-350 kHz) is considered low enough compared to the lower limit for the resonance frequency calculated in (8) in order to avoid exciting this resonance mode.

Another attenuation is due to the limited bandwidth of the high voltage amplifier (lab made) used to amplify the output of the signal generator (Agilent 33120A). Within the frequency range 150-350 kHz the attenuation varies between 0% and 4%. Hence, an average attenuation factor of  $\eta_2 = 0.98$  will be taken into account.

The effective displacement generated by the piezo actuator can now be calculated as:

$$\Delta z_{amp} = \eta_1 \eta_2 d_{33} U = 57 \text{ nm} \quad (9)$$

Hence, in order to obtain the minimum frequency for releasing a polystyrene sphere of  $\text{Ø}50 \mu\text{m}$  calculated above (i.e.  $8.99 \cdot 10^4 \text{ m/s}^2$ ) a sinusoidal signal with frequency of at least 199.9 kHz should be applied.

## V. MICRO MANIPULATIONS WITH AN INERTIAL MICRO GRIPPER

Experiments of micro manipulation with polystyrene balls of  $50 \mu\text{m}$  were conducted with the inertial micro gripper. Relative humidity was modified from 0% to 40% and two types of excitation signals were applied on the piezo element and their frequency was adjusted.

In the next section, minimal frequencies of release are measured as well as positioning repeatability and success rate. Pick and place operations are then evaluated by using a frequency threshold of 350 kHz. For the success rate evaluation, an operation is considered as a failure if the release was not possible or if the positioning error was higher than  $20 \mu\text{m}$ .

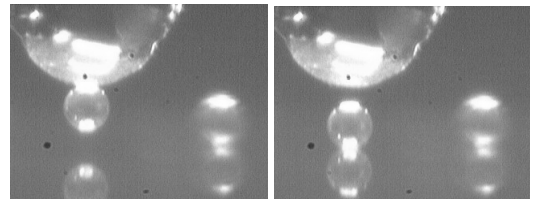


Fig. 4 Close view to the glass sphere end-effectors when catching and ejecting a  $50 \mu\text{m}$  polystyrene sphere.

### A. Picking a micro object

The glass substrate is mounted on a flexible structure with a stiffness of  $10 \mu\text{N}/\mu\text{m}$  in order to limit the force operated on the object (figure 5). It was observed that without this low stiffness, objects were crushed during the picking operation and that it was then necessary to apply an excessively high acceleration to release them or even impossible to release. This was certainly due to the fact that

the object was deformed and thus the contact surface grows implying a bigger adhesive effect.

As the adhesion forces on the substrate side and the end-effectors side are quite similar the operation of picking a part by using only adhesion is not enough efficient. Another solution consists in rolling the micro spheres between substrate and end-effectors. This method improves the conditions of pick and release as shown in [4]. Experiments have shown that it is sometimes the only way the catch the micro object and get a success rate of 75% at the first trial.

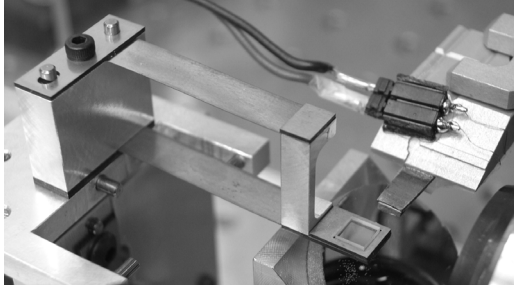


Fig. 5 Workspace in the micromanipulation setup with the substrate on the flexible system and the inertial micro gripper.

### B. Releasing experiments

Two kinds of excitation signals were applied on the piezo element. The first one was a single sine pulse and the second a pulse stream build from 10 sine pulses. Both were sent in burst mode ( $f_{burst} = 50\text{Hz}$ ).

1) *Minimal frequency of release*: Before using the inertial micro gripper tool for pick and place operations it is necessary to determine a frequency threshold. The experiments were carried out by increasing the frequency from 60 kHz to 350 kHz by steps of 10 kHz and measuring the minimal release frequency. Table II presents the results.

RH	Piezo signal	Average of the minimal frequency [kHz]	Variance [kHz]	Success rate
2%	1 imp	212.1	44.1	84.1 %
	10 imp	257.7	52.9	90.9 %
20%	1 imp	239.6	43.5	80.7 %
	10 imp	229.9	41.0	92.0 %
40%	1 imp	253.3	55.8	83.1 %
	10 imp	243.3	65.4	92.4 %

TABLE II

MEASURE OF THE MINIMAL FREQUENCY OF RELEASE FOR DIFFERENT RELATIVE HUMIDITY (RH) CONDITIONS AND EXCITATION SIGNALS.

RH	Piezo signal	Acceleration [ $\text{m/s}^2$ ]	Corresponding adhesive forces [ $\mu\text{N}$ ]	Variance [ $\mu\text{N}$ ]
2%	1 imp	$1.018 \cdot 10^5$	7.00	0.30
	10 imp	$1.446 \cdot 10^5$	9.93	0.44
20%	1 imp	$1.299 \cdot 10^5$	8.93	0.29
	10 imp	$1.196 \cdot 10^5$	8.22	0.26
40%	1 imp	$1.452 \cdot 10^5$	9.98	0.48
	10 imp	$1.340 \cdot 10^5$	9.21	0.67

TABLE III

CORRESPONDING FREQUENCIES AND ADHESIVE FORCES.

These frequencies can be used to compute the supplied acceleration (equation 5) and then the corresponding adhesive

forces ( $F_{adhesion} = \text{mass} \times \text{acceleration}$ ). The pull-off force computed in the last section based on the JKR model was  $6.48\mu\text{N}$ . Extracted values from measurements are well in the order of magnitude of the theoretical calculation. The light increase corresponds certainly to the increase of capillary effect with the increase of relative humidity (see table III).

2) *Positioning measurement*: Once a ball picked, it is placed  $5\mu\text{m}$  above the substrate and the position of the sphere is measured. The sphere is released and the position is measured again. The positioning error in x and y corresponds to the position after release minus the starting position. The frequency threshold is set to 350 kHz but the two kinds of excitation are still studied. This corresponds to an acceleration of  $2.773 \cdot 10^5 \text{m/s}^2$  and should be sufficient to counterbalance forces until  $19.1\mu\text{N}$ . Results are presented in table IV. Sources of positioning errors are the following:

- The balls were caught on the bottom of the end-effectors spherical tip, but errors still remain comparing to the center of the sphere.
- Electrostatic effects are also sometimes present at the release time inducing some attractive or repulsive effect on the substrate.
- The displacement of the piezo was made as perpendicular as possible to the substrate but there was no way to correctly measure this alignment and to precisely control it.

RH	Piezo signal	Position repeatability [ $\mu\text{m}$ ]	Success rate
2 %	1 imp	3.91	47.7 %
	10 imp	2.81	96.9 %
20 %	1 imp	4.75	73.3 %
	10 imp	5.92	92.6 %
40 %	1 imp	4.37	88.9 %
	10 imp	3.89	90.0 %

TABLE IV

POSITIONING REPEATABILITY MEASUREMENT WITH A FREQUENCY THRESHOLD OF 350kHz WITH DIFFERENT HUMIDITY CONDITIONS AND PIEZO SIGNALS.

The observed position repeatability is quite constant even when modifying the relative humidity and the signal. However operations are conducted successfully in less than 50% of the case when using a single impulsion signal and low relative humidity. The pulse stream sees here its main interest.

## VI. PASSIVE INERTIAL GRIPPER CONCEPTS

Having a piezo element as all other actuators on a gripper implies the use of connectors and wires between the tool and the gripper or the surroundings.

Three gripper concepts are presented here. In each case, the picking is realized with adhesion forces. The release occurs by the way of a shock, but requires no actuator: either the robot provides the energy needed for the release from its dynamics, or a passive system accumulate it.

### A. Using the manipulator dynamics

A spring element is inserted between the manipulator and a mass where is fixed the gripping element (figure 6). A fast sine movement is induced by the manipulator. While going upwards, and while the robot accelerates, a bump allows

driving the mass upwards (figure 6a). When the robot begins to decelerate, the inertia of the mass drives itself upwards (figure 6b). Due to the spring restoring force and the gravity the mass falls back, a shock occurs and the object is released (figure 6c).

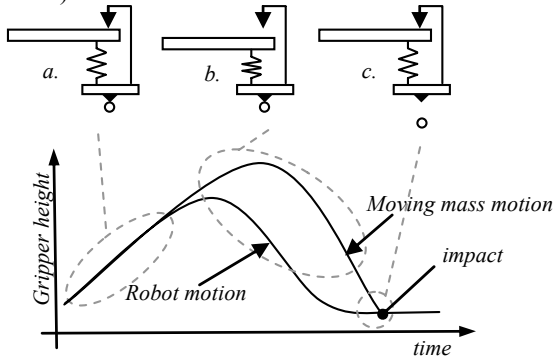


Fig. 6 Principle sketch of an inertial gripper using the dynamics of the robot.

### B. Using both adhesion on the substrate and inertia

In this scenario the picked object is placed in contact on the release target. Then the gripper is shocked upwards. The inertia of the object added to the adhesion force between the object and the substrate counterbalance the adhesion force between the object and the gripper, allowing the release of the object.

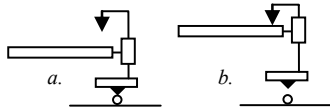


Fig. 7 Once the part is centred and in contact with the substrate, the robot is then driven quickly upwards until it leads away the gripper tip.

### C. Using a stressed spring as energy stock

The gripping tip is attached to a "spring – mass" system. The spring is constrained and then released on a bump. The release of the object is done as it continues its way due to its inertia (fig. 8). The energy stored in the stressed spring will be transferred to the object as kinetic energy. This energy will counterbalanced the adhesion between the object (in our case a PS sphere).

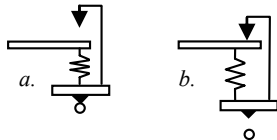


Fig. 8 The spring is first constraint (a). Once released, the system slaps against a bump (b).

In order to determine the spring stroke needed for release, the adhesion was modelled in term of energy using the interaction potential between a sphere and a plane, as:

$$E_{ad} = \frac{A \cdot R}{6D_0} \quad (10)$$

where A is the Hamaker constant,  $D_0$  the distance between the object and the gripper, and R the radius of the object.

A first prototype has been developed at LSRO in order to validate the concept, as pictured on fig. 9. Successful releases

were operated but with higher spring constrains than expected inducing thus an upgrade of the model as the next step.

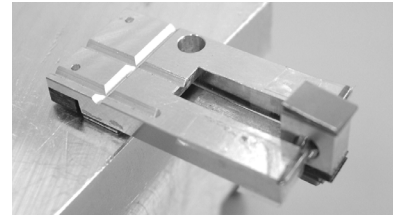


Fig. 9 Prototype of passive inertial gripper based on a stressed spring.

## VII. CONCLUSION

This paper presents a micro gripper based on adhesive gripping and inertial releasing. Experiments have demonstrated that this tool is reliable as shown by the success rate of precise releasing of more than 90% in environment with relative humidity of 40% and less. The use of adhesion as catching principle was valuable when manipulating balls especially when the rolling method was used. However manipulation of cubic or with non defined shapes micro object will ask to improve the catching process.

The quantification of the adhesive effect by the use of such a tool would be effective within the condition that the contact surface should be well defined and that the overall attenuation of the acceleration by the tool itself is clearly known. Still it was already possible to extract a slow tendency along the modification of the relative humidity.

The integration of this kind of tool on an assembly cell would ask however to care about the crushing force. This last one has to be limited in order to not increase inconsiderably the necessary releasing acceleration. Placing the conveyor or stock on a flexible support becomes mandatory unless the tool is mounted itself with a force limitation device, which should not disturb the inertial process.

## ACKNOWLEDGMENT

The authors would like to acknowledge Julien Moulin for his precious contribution on the experiments of the inertial micro gripper.

## REFERENCES

- [1] J. Agnus, P. Nectoux, N. Chaillet, "Overview of microgrippers and design of a micromanipulation station based on a MMOC microgripper", in *Computational Intelligence in Robotics and Automation*, 2005.
- [2] S. Saito, H. T. Miyazaki, T. Sato, K. Takahashi, T. Onzowa, "Dynamics of micro-object operation considering the adhesive effect under a SEM", in *Microrobotics and Microassembly III*, 2001.
- [3] D.S. Haliyo, S. Régner, J.-C. Guinot, "[mü]MAD, the adhesion based dynamic micro-manipulator", *European Journal of Mechanics –A/Solids*, 22, 2003, pp. 903-916.
- [4] W. Driesen, T. Varidel, S. Régner, J.-M. Breguet, "Micro manipulation by adhesion with two collaborating mobile micro robots", *J. Micromech. and Microeng.*, 15, 2005, pp. 259-267.
- [5] M. Dafflon, B. Lorent, R. Clavel, "A micromanipulation setup for comparative tests of microgrippers", in *International Symposium on Robotics (ISR)*, 2006.
- [6] K.L. Johnson, K. Kendall, A.D. Roberts, "Surface energy and the contact of elastic solids", *Proc. R. Soc. Lond. A.*, 324, 1971, pp. 301.